Scanning Microscopy

Volume 3 | Number 4 Article 2

11-3-1989

Scanning Electron Microscope with a Single-Polepiece Lens

V. Kolařík
Czechoslovak Academy of Sciences

I. Müllerová
Czechoslovak Academy of Sciences

M. Lenc
Czechoslovak Academy of Sciences

Scanning Microscopy, Vol. 3, No. 4, 1989 (Pages 1003-1008) 0891-7035/89$3.00+.00
Scanning Microscopy International, Chicago (AMF O'Hare), IL 60666 USA

SCANNING ELECTRON MICROSCOPE WITH A SINGLE-POLEPIECE LENS

*V. Kolařík, I. Müllerová, M. Lenc

Institute of Scientific Instruments, Czechoslovak Academy of Sciences, 612 64 Brno, Czechoslovakia

(Received for publication March 25, 1989, and in revised form November 03, 1989)

Abstract

The design of an ultra-high vacuum scanning electron microscope (UHV SEM) with a single-polepiece lens underneath the specimen is described with the possibility to guide backscattered (BSE) and secondary electrons (SE) which originate in the magnetic field of the single-polepiece lens to the detectors. Our new design of the single-polepiece lens and in-lens deflection coils closely satisfy the condition of a variable axis immersion lens (VAIL), which results in very low deflection aberrations.

KEY WORDS: Single-polepiece lens, Variable axis immersion lens, Deflection aberrations.

*Address for correspondence:
V. Kolařík
Institute of Scientific Instruments, Czechoslovak Academy of Sciences, 612 64 Brno, Czechoslovakia
Phone: 42 - 5 - 749292

Introduction

The use of the single-polepiece lens (Mulvey, 1982) as a scanning electron microscope objective lens offers several interesting advantages. The good electron optical parameters, especially the low chromatic and spherical aberration coefficients, are well known (Hill and Smith, 1982) and they hardly increase with the number of the intermediate images employed (Lenc and Müllerová,1988). A number of interesting results can be obtained by the detection of back-scattered electrons (BSE) and secondary electrons (SE) which originate in the magnetic field of the single-polepiece lens. Magnetic parallelization i.e. the reduction of beam divergence is increasingly used for energy analysers, for E-beam testers (Kruit and Dubbeldam, 1987) or for electron spectroscopy (Kruit and Venables, 1988). Bode and Reimer (1985) used a single-polepiece lens for the detection of BSE.

We studied in more detail the detection of BSE by using a single-polepiece lens (Müllerová et al, 1989). Here we are concerned with the design of a modified Variable Axis Immersion Lens (VAIL) in scanning electron microscope (SEM), so as to be able to deflect the primary beam across the specimen surface at normal incidence or, for stereoscopic work for example, at an inclined angle to the surface. We designed the single-polepiece lens and in-lens deflection coils so that their calculated flux densities closely satisfy the condition of a Moving Objective Lens (MOL).

We calculated the coma, field curvature and astigmatism of the system as set out below.

The design of a UHV SEM with a single-polepiece lens

In our SEM we decided to use a field emission electron gun with a magnetic lens operating with a TF-W/100-Zr cathode in the 1 - 100 kV range (Delong et al, 1989). This gun has been working in our experimental SEM (accelerating voltage 1 - 25 kV) for more than one year without problems.

The design of the UHV SEM column with a single-polepiece lens is shown in Fig. 1. The column consists basically of two lenses, an intermediate lens 3 and the single-polepiece lens 11, 12 with two systems of deflection coils (predeflection coils 4, 5 and in-lens deflection coils 10).

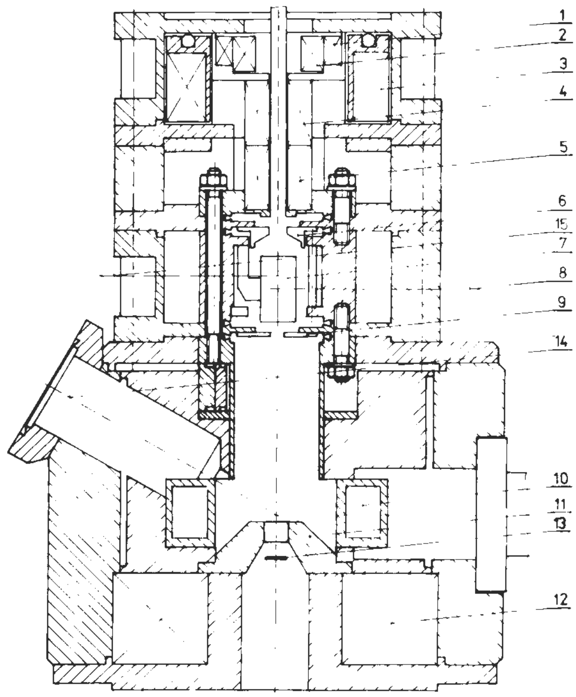

Fig. 1: Detailed design of the ultrahigh vacuum SEM with a single-polepiece lens. 1. stigmator coils, 2. beam centering coils, 3. intermediate lens, 4.5. two-stage predeflection coils, 6. auxiliary BSE detector, 7. crossed field deflector, 8. SE detector axis, 10. cross section of a pair of toroidal in-lens deflection coils, 11. polepiece of final lens, 12. excitation coil of the single-polepiece lens, 13. transmitted electron detector, 14. energy dispersive X-ray detector, 15. exit port of Auger electron detector.

The field emission gun is not shown in the Figure.

We have used the single-polepiece lens as a scanning electron microscope objective lens to guide the SE and BSE to the detectors by means of its magnetic field. This enables us to detect nearly all BSE and to have sufficient free space above the specimen for the in-lens deflection coils. We can get a wide range of angles of incidence for the primary beam using the proper adjustment of the predeflection and the in-lens deflection coils. In future we would like to make use of the parallelization of SE trajectories for good energy spectroscopy (Garth and Nixon, 1986) and for Auger spectroscopy (Kruit and Venables, 1988). For the detection of SE, Auger electrons and the paraxial BSE we intend to take advantage of the use of a crossed field deflector 7 with the value and orientation of the crossed magnetic and electric fields so that the deflector will not influence primary beam electrons so that secondary and paraxial backscattered electrons moving in the opposite direction will be deflected to the detectors.

So far we have performed only basic experiments with the SE detection, but we studied more in detail the detection of the BSE. We used semiconductor detectors for detection of BSE and would like to use one also for the detection of transmitted electrons (TE). Our set-up of the SEM is also appropriate for a windowless X-ray energy dispersive detector 14 because no parasitic electrons strike the detector.

VAIL concept for the use in SEM

The concept of MOL was first described by Ohiwa et al. (1971). To fulfil the MOL condition properly, a system is required (see Fig. 2a) with the first lens in front of the predeflection coil and the second (final) lens in a telescopic mode

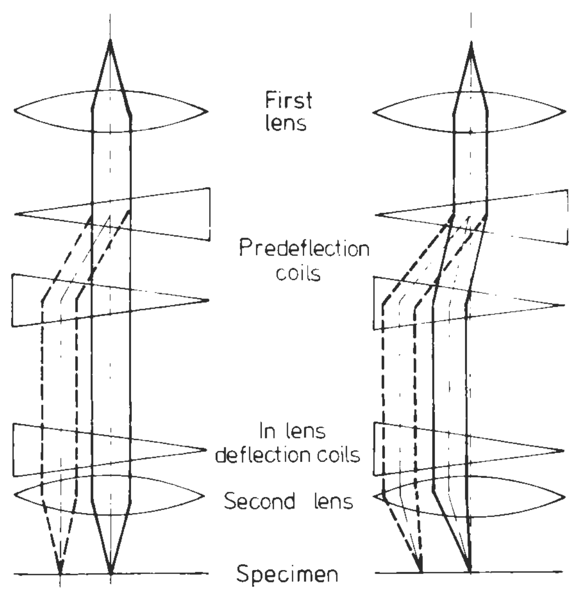

Fig. 2: a) Standard Variable Axis Immersion Lens and b) VAIL with a tilted beam.

with the first one, a two-stage predeflection system shifting the beam parallel to the axis and in-lens deflection system in the final lens. The axial flux density destribution D(z) of the in-lens deflector should be of the form D(z) = const B' (z), where B(z) is the axial flux density distribution of the final lens. The complex constant given by the strength and the orientation of the in-lens deflectors is chosen so that the shifted beam is not further deflected as it passes through the final lens. The Variable Axis Lens (VAL) was introduced by Pfeiffer and Langner (1981) who set out its theory, construction and experimental results. If the specimen is immersed in the magnetic field of the lens (Variable Axis Immersion Lens - VAIL), the in-lens deflection system consists of a single deflector. A detailed and clear description of VAIL was given by Pfeiffer and Sturans (1985).

For the application in SEM, the VAIL shows several advantageous properties. The first one has been mentioned by Kruit and Venables (1988): in VAIL the magnetic flux line that goes through the point where the primary beam is incident onto the specimen is parallel to the optical axis, thus SE are parallelized along the optical axis.

In this paper we would like to point out another important advantage. It is possible to obtain very high angles of incidence for the primary beam without seriously disturbing the resolution and without introducing large distortion. This possibility arises from the low spherical aberration and zero deflection coma of the VAIL. For the third-order aberration in the Gaussian image plane (the magnification of the final lens is M=0) there holds

$$\delta w(z_i) = k_S\alpha^2\bar{\alpha} + K_L\alpha\bar{\alpha}\gamma + 1/2.\bar{K}_L\alpha^2\bar{\gamma} + K_F\alpha\gamma\bar{\gamma} + K_A\bar{\alpha}\gamma^2 + K_D\gamma^2\bar{\gamma} \qquad (1)$$

where k_S is the spherical aberration coefficient, and the deflection aberrations are K_L, K_F, K_A and K_D for coma length, field curvature, astigmatism and distortion, respectively. As usual α stands for the beam semi-aperture and γ for the deflection. Bars denote complex conjugates.

Now if a constant shift of the beam parallel to the axis is introduced by means of the predeflection coils (Fig. 2b), the optical axis of the lens is shifted either more or less than necessary for the exact matching with predeflected beam i.e. for the exact matching the condition of MOL. In this way we still have the beam scanning the specimen surface with a constant angle ψ with respect to the optical axis, but the beam no longer impinges perpendicularly. In the aberration expression (1) we substitute $\alpha \pm \psi$ for α in all terms. The terms $k_S\ (\psi^2\bar{\psi} + 2\psi\bar{\psi}\alpha + \psi^2\bar{\alpha})$ can be compensated by a slight constant shift, defocusing and a stigmatic correction of the primary beam, respectively. The resolution can be estimated now using the expression

$$|\delta w| \doteq 3|k_S\alpha^2\psi| + 3|K_L\alpha\psi\gamma| + |k_S\alpha^3| + 3/2|K_L\alpha^2\gamma| + (|K_F| + |K_A|)|\alpha\gamma^2| \qquad (2)$$

and the distortion by expression

$$|\delta w| \doteq 3/2|K_L\psi^2\alpha| + (|K_F| + |K_A|)|\psi\gamma^2| + |K_D\gamma^3| \qquad (3)$$

Considering typical values $\alpha = 5.10^{-3}$ and $\gamma_0 = 1$ mm and a reasonable value of ψ about 15^o, $\psi = 2{,}5.10^{-1}$, one can see from (2) and (3) how dramatically both the resolution and the distortion can deteriorate. If the VAIL incorporates dynamic focus coils with axial flux density proportional to B'' (z) (as described, for example, by Pfeiffer and Sturans (1985)) one finds that besides $K_L = 0$, $K_F = 0$ also, and with dynamic stigmator coils with axial flux density distribution proportional to B''' (z), K_A is actually zero. According to (3) there is no additional distortion for non-zero ψ and according to (2) the resolution is worsened only by the term corresponding to the second order axial coma. But even without dynamic corrections, the VAIL has very low field curvature and reasonably small astigmatism (Lencová (1988)).

Constructional details and lens calculations

The essential detail of the final lens arrangement is shown schematically in Fig. 3. The dimensions of the yokes of the toroidal deflection

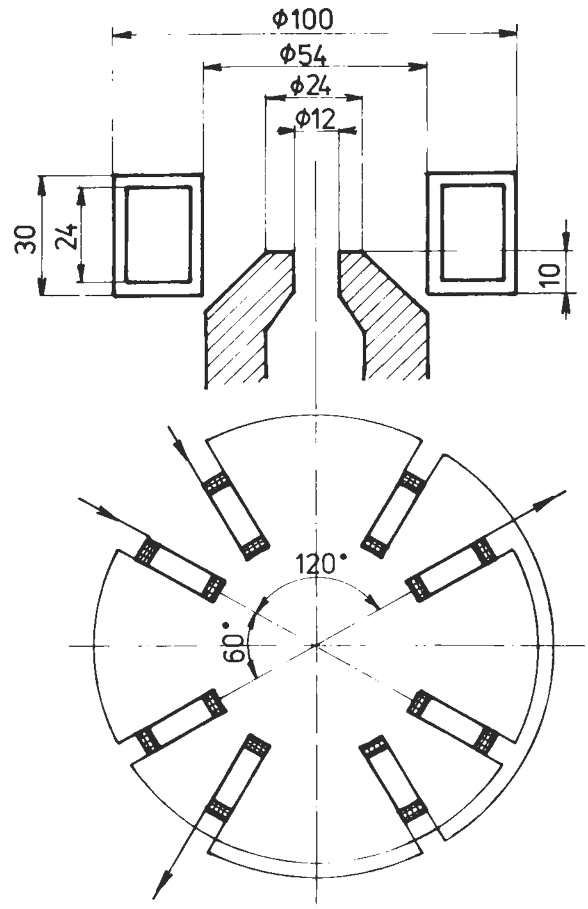

Fig. 3: Upper diagram: Schematic arrangement of the essential features of the final lens polepiece and a section through two of the toroidal deflection coils. Lower diagram: Plan view of the toroidal deflector coils above the final lens polepiece, showing electrical connections. Dimensions in mm.

coils are determined by the condition that there must be free access to the specimen in several sectors of the solid angle (for energy dispersive X-ray detectors, ion guns, specimen stage movements etc.). The dimensions of the polepiece of the single-polepiece lens are set by the following two considerations. The maximum flux density should occur in the specimen plane about 5 mm above the polepiece tip. The derivative of the flux density distribution should be relatively small for two reasons: (i) to ensure the adiabaticity of the motion of SE and (ii) to produce a reasonably large field of view in the VAIL arrangement.

Fig. 4 shows normalized axial flux density distributions $B(z)/B_{max}$, its normalized derivative $B'(z)/B'_{max}$ and the normalized deflector flux density $D(z)/D_{max}$, respectively. The corresponding absolute values are: $B_{max} = 4.44.10^{-2}$ T for an

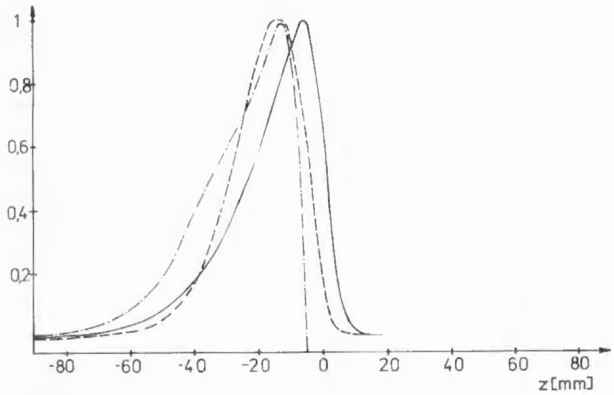

Fig. 4: Normalized axial flux density distribution. Solid line: $B(z)/B_{max}$, chain dotted: $B'(z)/B'_{max}$ and dashed: the deflector flux density $D(z)/D_{max}$.

excitation of 1000 ampereturns (A-t) at a distance $z = 5.3$ mm above the polepiece top, $D_{max} = 8.4\ 10^{-5}$ T for an excitation of 50 A-t at a distance $z = 13.7$ mm above the polepiece and $B'_{max} = 1.51\ 10^{-3}$ T mm^{-1} for of 1000 A-t at a distance $z = 11.8$ mm above the polepiece. From Fig. 4 it follows that there is substantial proportionality between $B'(z)$ and $D(z)$.

For an excitation parameter $NI/(V)_r^{1/2} = 16\ AV^{-1/2}$ (where NI is the lens excitation and V_r is accelerating voltage) the lens is focussing from infinity into the plane of the maximum flux density (specimen plane). The objective focal length is f= = 14.8 mm, the spherical aberration coefficient $C_s = 5.8$ mm and the chromatic aberration coefficient $C_c = 9.8$ mm.

Fig. 5 shows curves representing the dependence of the deflection aberration coefficients (coma, field curvature, astigmatism) on the relative orientation of the predeflection shifting coils (two identical stages of toroidal coils with opposite excitation) and the in-lens deflection coils from Fig. 3. The values of the field curvature and astigmatism at the zero value of coma are also reasonably small.

For the optimum case ($K_L = 0$) the maximum value of the actual deflection flux density distribution D(z) is 1.88 times higher than for the ideal case and the angular displacement with respect to the predeflection is 47^o instead of 90^o.

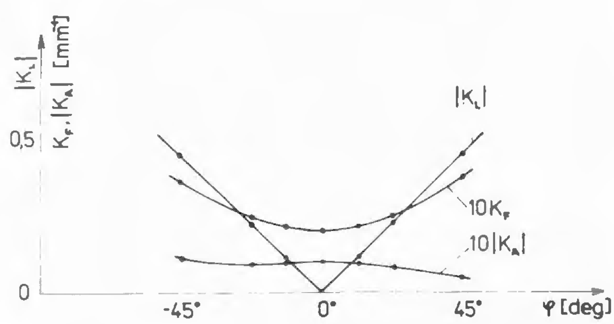

Fig. 5: The dependence of the deflection aberration coefficients (coma length K_L, field curvature K_F and astigmatism K_A) on the relative orientation of the predeflection and in-lens deflection coils φ.

The description of the methods used for the numerical calculations can be found in the papers by Lencová and Lenc (1986) and Lencová (1988).

An excitation of about 50 ampereturns of the in-lens deflection coils provides a 0.1 mm field of view for 15 keV primary beam energy.

Conclusion

In this paper the design of the analytical SEM with a single-polepiece lens and tilted-beam VAIL has been described. The aberrations caused by the tilted beam are very low but corrections for shift, defocussing and axial astigmatism are necessary. This means, for example, that for rocking beam methods the above-mentioned corrections must be applied dynamically. Several basic design principles have been verified experimentally (telescopic mode with the first lens and the single-polepiece lens, efficient detection of BSE and SE, long-term performance of the field emission gun). The classical solution of the in-lens deflection coils (Teflon yokes and 15 to 20 turns of isolated wire) is quite satisfactory for experimental work, but a true ultrahigh vacuum design will be necessary for a routine analytical SEM.

The efficient energy analysis of all kinds of electron signals will be possible in the near future.

References

Bode M, Reimer L (1985) Detector strategy for a single-polepiece lens. Scanning 7:125-133.

Delong A, Chmelík J, Kolařík V, Komůrka J, Očadlík J (1989) A new design of the field emission electron gun with a magnetic lens. Optik 81: 103-108.

Garth SCJ, Nixon WC (1986) Magnetic field extraction of secondary electrons for accurate integrated circuit voltage measurement. J. Vac. Sci. Technol. B4:217-220.

Hill R, Smith KCA (1982) The single-polepiece lens as a scanning electron microscope objective. Scanning Electron Microsc. 1982; II:465-471.

Kruit P, Dubbeldam L (1987) An E - beam tester with dispersive secondary electron energy analyser Scanning Microsc. 1:1641-1646.

Kruit P, Venables JA (1988) High-spatial-resolution electron spectroscopy. Ultramicroscopy 25: 183-193.

Lenc M, Müllerová I (1988) Efficient collection of BSE with single-polepiece lens. EUREM 88 York England I:117-118, Inst. Physics, Bristol, U.K.

Lencová B, Lenc M (1986) A finite element method for the computation of magnetic electron lenses. Scanning Electron Microsc. 1986; III:897-915.

Lencová B (1988) On the design of electron beam deflection systems. Optik 79:1-12.

Müllerová I, Lenc M, Florián M (1989) Collection of backscattered electrons with a single polepiece lens and a multiple detector. Scanning Microsc. 3, 419-428.

Mulvey T (1982) Unconventional lens design, in: Magnetic Electron Lenses (ed.) Hawkes PW Springer Berlin Heidelberg New York:360-412.

Ohiwa H, Goto E, Ono A (1971) Elimination of third-order aberrations in electron-beam scanning systems. Electr. Commun. Japan 54B:44-51.

Pfeiffer HC, Langer GO (1981) Advanced deflection concept for large area, high resolution e-beam lithography. J. Vac. Sci. Technol. 19:1058-1063.

Pfeiffer HC, Sturans MA (1985) Electron beam deflection without off-axis aberrations, in: Electron Optical System SEM Inc. AMF O'Hare (Chicago): 109-114.

Discussion with Reviewers

P. Kruit: Is the conclusion that "there is no additional distortion for non-zero angle ψ according to (2) and the resolution..." not a little premature? You need to compensate dynamically for 5 terms plus the field of the VAIL coils has to fit the first, second and third derivatives of B(z) exactly! Do you have any experimental evidence that these large rocking angles will be possible?

Authors: For the rocking beam mode of scanning (the angle ψ scanned) it's necessary to compensate dynamically for five terms. For the normal scanning mode (the angle ψ constant) we need to compensate dynamically for two terms only. But we don't intend to use the dynamic correction for the minimum values of the aberration coefficients from Fig. 5 at all. The distortion is below 1% for $|\gamma|$ = 1 mm and $|\psi|$ = 0.25. We have an experimental evidence for the low value of distortion but using the present experimental system we are not able to demonstrate the negligible dependence of the resolution on the angle ψ .

T. Mulvey: Can you supply more detail about the arrangements for collecting the secondary electrons through the lens under VAIL conditions? What sort of collection efficiency does your system have? When using tilted - beam VAIL, is the SE collection efficiency constant over the entire field of view?

Authors: The position of the SE detector and its collection efficiency were not optimized. We have not studied more detailed collection of the secondary electrons through the lens under VAIL conditions yet. But the illumination of the field of view 3 x 3 mm^2 was uniform even when we used tilted-beam VAIL.

P. Kruit: The use of intermediate images, or cross-overs, inside the field of the objective lens might well become an important issue in low energy SEM. I even think that there are situations in which the axial aberrations decrease when going to one or two intermediate cross-overs. However, the deflection aberrations will probably increase dramatically. Have the authors performed any calculations on the deflection aberrations for the multiple intermediate crossovers situation in their instrument?

Authors: The values of the deflection coefficients are not generally increasing with the number of intermediate images. This is illustrated in Table 1, where the values for 1, 2 and 3 images are given. The object plane is at infinity, the image plane in the position Z = -5.31 mm of the maximum of the single-polepiece lens flux density distribution (B_{max} = 0.061 T). The excitation and the orientation of the in-lens deflection coils are chosen so that the zero coma condition (Re K_L = Im K_L = 0) is satisfied. The deflection in the image plane c = 1 mm. For the exact VAIL the predeflection c_p = c = 1 mm, $\varphi = -90^0$ and $D_{max} = 1/2\, c_p B'_{max}$ = 0.00104 T, and also Re K_T = Im K_T = 0.

Table 1: The comparison of the performance of the deflection system for 1, 2 and 3 images. V_r - accelerating voltage in V, n - number of images, c_p- predeflection in mm, φ - angular displacement of the in-lens coils with respect to the predeflection coils in degrees, D_{max}- the maximum value of the in-lens coils deflection flux density in T, K_A, K_F and K_D - the deflection aberrations coefficients of the astigmatism, field curvature and distortion in mm^{-1} , mm^{-1} and mm^{-2} respectively. K_T - the coefficient of the chromatic aberration of deflection (dimensionless).

V_r	7383.7	1278.7	506.5
n	1	2	3
c_p	0.71	0.37	0.30
φ	-46.9	-38.0	-51.1
$10^4\ D_{max}$	13.8	16.4	16.6
$10^3\ K_A$	-9.80+1.78i	1.79+3.30i	-0.52+1.28i
$10^2\ K_F$	2.05	1.33	1.62
$10^4\ K_D$	-0.65-6.59i	-0.11+6.71i	-1.26+3.54i
$10^2\ K_T$	7.86-3.88i	2.21-6.66i	0.94-4.37i

S. Golladay: The match of correction yoke field D(z) to the lens field derivative B'(z) is not very exact due to the position of the yoke coils outside the pole pieces. In view of this mismatch do the authors have any data about how well constant landing angle can be maintained over the entire deflection field?
Authors: Owing to the mismatch mentioned in the question, the condition for the landing angle to be maintained constant over the entire deflection field is not satisfied at the same time as is the zero coma condition. Even in that case the landing error is still small, $|c'(z_i)/c(z_i)| < 1.10^{-2}$.
T. Mulvey: What do you see as the chief operational advantage of tilted-beam VAIL?
Authors: 1.The possibilities of producing stereoscopic pictures with a quality given by VAIL conditions. 2.To get clear channeling contrast under the angles chosen.
P. Kruit: How does the specimen stage fit in the design?
Authors: The specimen stage is considered to be of "side entry" type similar in design to that commonly used in TEM. The connection of the supporting flange of the table with one of four input ports perpendicular to the optical axis will be implemented in UHV technique. It is also assumed that the vacuum air-lock to allow inserting of the specimen, will be an integral part of the whole mechanism.